Fuel Kinetic Effects on Pre-Spark Heat Release and Engine Knock Limit

A. Gilliam[1], D.A. Splitter[2], J.P. Szybist[2], and J.B. Ghandhi[1]

[1]University of Wisconsin – Madison Wisconsin. 1500 Engineering Drive, 53712, USA.

E-mail: jaal.ghandhi@wisc.edu
Telephone:+(1) 6082631684

[2]Oak Ridge National Laboratory. USA

E-mail: splitterda@ORNL.gov
Telephone: +(1) 8659461347

Abstract. This study focuses on the ability of chemical mechanisms to describe the recently discovered phenomena of pre-spark heat release (PSHR) due to low-temperature chemistry. Experiments were conducted at fixed air and fuel flow rates for a range of intake temperature that spanned the threshold for PSHR. It was found that when PSHR occurred, the knock-limited combustion phasing was insensitive to intake temperature. A three-zone model using full chemistry was used to investigate the phenomenon with both a detailed and skeletal chemical kinetic mechanism. Both mechanisms predicted the presence of PSHR. The skeletal mechanism was found to more faithfully reproduce the experimentally observed phasing of the PSHR with intake temperature at the two speeds investigated. The model results showed that end gas heat released was observed even for conditions for which the PSHR was not observed, i.e., the low temperature heat release in the end gas was obscured by the deflagration heat release. The chemical change to the unburned zone would affect both the mixture flame sped and autoignition characteristics. The model results were used to explore regions where PSHR would be found.

Notation (optional)

RON	*Research Octane Number*
MON	*Motor Octane Number*
S	*Octane Sensitivity*
SI	*Spark Ignited*
CFPH	*Central Fuel Property Hypothesis*
NTC	*Negative Temperature Coefficient*
LTHR	*Low Temperature Heat Release*
PSHR	*Pre-Spark Heat Release*
IMEP	*Gross Indicating Mean Effective Pressure*
LLNL	*Lawrence Livermore National Laboratory*
NO	*Nitrogen Oxide*
RK	*Rein and Kokjohn*
KLSA	*Knock Limited Spark Advance*
CAD	*Crank Angle Degrees*
TDC	*Top Dead Center*
dATDC	Degrees After Top Dead Center Firing
r/min	*Revolutions per Minute*
IVC	*Intake Valve Closing*

This manuscript has been authored by UT-Battelle, LLC, under Contract No. DE-AC0500OR22725 with the U.S. Department of Energy. The United States Government retains and the publisher, by accepting the article for publication, acknowledges that the United States Government retains a non-exclusive, paid-up, irrevocable, world-wide license to publish or reproduce the published form of this manuscript, or allow others to do so, for the United States Government purposes. The Department of Energy will provide public access to these results of federally sponsored research in accordance with the DOE Public Access Plan (http://energy.gov/downloads/ doe-public-access-plan).

1. Introduction

The US Department of Energy Co-Optimization of Fuels and Engines ("Co-Optima") initiative aims to foster the co-development of advanced fuels and engines for higher efficiency and lower emissions (Szybist & Splitter, 2018). A guiding principle of Co-Optima is the central fuel properties hypothesis (CFPH), which states that fuel properties provide an indication of the performance and emissions of the fuel, regardless of the fuel's chemical composition. CFPH is important because many of the candidate fuels being investigated in the Co-Optima initiative are bio-derived compounds with oxygen-containing functional groups typically not associated with commercial transportation fuels. The purpose of this investigation is to determine if fuel having the same properties exhibit different knocking behavior. The present work is the calibration case using isooctane, which is part of a larger study investigating if a wide range of fuels at constant research octane number (RON), with varying fuel molecular type, exhibit different high-load knocking behaviour and limits with boosted engine operation spanning intake temperatures between the RON and motor octane number (MON) conditions. This information will be useful in determining not only the merit of the CFPH but also for identifying abnormal combustion phenomena that could be fuel specific in follow-on studies and analysis.

Spark ignition (SI) engine efficiency and operation are fundamentally limited by knock, a process observed via cylinder-pressure measurements as early as the late 1910's (Splitter, et al., 2016). Knock is an unwanted and uncontrolled autoignition of the fuel, which if not avoided can lead to engine damage, and therefore is impermissible in almost all engine applications. Although knock is a fundamental barrier and has been studied for over a century, a fully detailed understanding of knock and other autoignition phenomena has proven elusive. Knock continues to be the primary barrier to achieving higher efficiency in SI engines, and the recent automotive trends of downsizing and downspeeding engines have exacerbated the issue. Therefore, improving the understanding of knock and fuel-specific effects on knock remain a high priority in engine and combustion research. Knock is highly fuel dependent; octane number tests are used to define a fuel's knocking tendency relative to reference fuels (isooctane and n-heptane, both alkanes).

One of the most insightful understandings of knock was presented by Leppard (Leppard, 1990), who showed that for alkanes, there is a two-stage ignition process: low-temperature heat release (LTHR) is followed by a negative temperature coefficient (NTC) region wherein the reaction rate becomes inversely proportional to temperature, and finally a high-temperature heat release event. The chemical origins and dependencies of the two-stage ignition process were more fully elucidated in the development of chemical kinetic mechanisms for the primary reference fuels, n-heptane (Curran, et al., 1998) and iso-octane (Curran, et al., 2002). Recently, the chemical origins of the two-stage ignition process of alkanes described by Leppard have been studied by Westbrook et al. (Westbrook, et al., 2016), who illustrated that molecular-specific effects on local electron destabilization is the most likely mechanism for LTHR reaction pathways in alkanes.

Many fundamental studies in shock tubes and rapid compression machines have been carried out on the fuel kinetic processes of LTHR, but to date much of the understanding and observation of LTHR in engines has come from compression ignition combustion processes, with many being kinetically controlled (e.g., homogeneous charge compression ignition (Najt & Foster, 1983). Rooney et al. (Rooney, et al., 1991) showed that at conditions spanning between RON to beyond-MON in a production engine alkane fuels could exhibit NTC reactions in the bulk gas, which could possibly be used to extend the lean operating limit. More recently findings by Yamakawa et al. (Yamakawa, et al., 2011), and Szybist and Splitter (Szybist & Splitter, 2017) have illustrated that LTHR processes also occur in stoichiometric SI engines when operated with both gasoline-like fuels and isooctane at relatively high loads and temperatures, i.e., conditions and fuels that are relevant to modern downsized SI engines. One finding from both studies was that LTHR can occur in SI engines before spark discharge, where Szybist and Splitter suggested that the process of pre-spark heat release (PSHR) was a low-temperature bulk gas combustion process, and both (Yamakawa, et al., 2011) and (Szybist & Splitter, 2017) observed a reduced knocking propensity as a function of intake temperature when PSHR occurred. The ramification of PSHR on knock are not fully understood, but these initial studies suggested that the knocking process is much less sensitive to intake temperature when PSHR occurs; therefore, reliance on conventional knock mitigation strategies like combustion retard are reduced when PSHR occurs, offering the potential for a high-load SI engine efficiency benefit.

In the present study we seek to expand the understanding of the role LTHR and PSHR on knock, by studying the knock propensity of neat isooctane fuel over a wide range of intake temperatures at knock prone conditions. The results are analyzed as functions of PSHR and intake temperature independently and also are compared with constant volume ignition delay simulations to support the observed trends. The results of this study highlight the importance of low temperature heat release processes on knocking propensity, and the corresponding effect that PSHR has on bulk gas kinetic state

and knock. Throughout the study the objective explored is to expand the understanding of the pre-spark heat release phenomena through detailed chemical kinetic modeling of the process, which takes into account the cumulative effect of the finite time spent in regions of relatively long ignition delay especially in regions where low temperature heat release occurs. The present preliminary results and novel approach and calibration with isooctane will be used as a baseline for applying the approach to a larger data set which includes a wide range of fuels that are part of the Co-Optima program, but to avoid uncertainty in the surrogate representation of these fuels, the present study focuses only on isooctane.

1. Experimental Apparatus

The experimental apparatus and much of the methodology used in this study have been previously reported (Szybist & Splitter, 2017). A 2.0 L General Motors Ecotec LNF engine equipped with the production side-mounted direct injection fueling system was used for this investigation. Engine geometry details are presented in **Error! Reference source not found.**. The engine was converted to a single-cylinder engine by disabling cylinders 1 – 3. The combustion chamber geometry and camshaft profiles were unchanged from the stock configuration. The engine has a camshaft phasing system, with camshaft position recorded from the production hall-effect sensors. A Kistler 6125C piezoelectric pressure transducer was flush mounted in the cylinder and an AVL 365C optical encoder was used to collect data at 0.2 CAD resolution. Intake air with less than five percent relative humidity was supplied to the engine and metered through an Alicat Scientific 2000 SLPM mass flow controller. Intake air was heated with a Sylvania Sureheat Max controller. Fuel was supplied by a pneumatically actuated, positive-displacement, high pressure pump. Fuel injection timing was held constant at 280 CAD before firing top dead center. Equivalence ratio was monitored by UEGO sensors mounted in both the intake and exhaust streams. All experiments conducted in this study were with neat PRF grade isooctane fuel supplied from Haltermann Solutions.

Table 1. Engine Geometry

Bore x Stroke	mm	86 x 86
Connecting Rod Length	mm	145.5
Compression Ratio	-	9.2:1
Wristpin Offset	mm	0.8

The intake temperature was swept from 40ºC to the maximum allowable temperature for the condition, as defined below. Tests were carried out at both 1000 r/min and 2000 r/min, and the knock-limited spark timing was used for each intake temperature. The intake air mass flow rate was held constant for each condition, 500 g/min at 1000 r/min and 1000 g/min at 2000 r/min, which resulted in intake pressures of 1.5 to 1.9 bar depending on the intake temperature. The equivalence ratio was unity for all the testing. The cam phasers were held in a constant position for both speeds to maintain constant intake valve closing (-142 dATDC) and exhaust valve opening (143 dATDC) timings. The fuel injection timing (-280 dATDC) and spark dwell was held constant with the stock ignition coil at 1.8 ms to maintain constant ignition energy. Engine fuel flow was measured with a Coriolis fuel flow meter, and cross checked with a laboratory grade wideband oxygen sensor installed in the engine exhaust. Throughout the study engine coolant and sump oil temperatures were maintained at 90 and 95°C, respectively. Under these operating conditions, the gross indicating mean effective pressure (IMEP) was in the range of 14-19 bar.

For a given intake temperature, the spark timing was set to the knock-limited spark advance and a data record of 5000 cycles was taken. After 5000 cycles were taken, the spark was momentarily disabled for the acquisition of a hot-motored cycle. Once the record concluded, timing was retarded for engine safety and the intake temperature was increased. The process repeated until the maximum allowable intake temperature was found, which was determined by the engine exhibiting pre-ignition events leading to heavy knock and/or superknock with a lack of ability to further retard the spark timing.

2. Physical and Chemical Models

2.1 Engine model

The engine was modelled using a three-zone model and the Cantera open-source solver. The three zones comprised the unburned and burned mixtures, for which the full chemical species evolution was computed, and a chemically inert crevice region. The crevice region was assumed to have a volume of 2% of the TDC volume of the engine and was maintained at the wall temperature through a high heat transfer rate. The crevice was fed from the unburned zone, and returned mass to the burned zone. The inclusion of the crevice was found to be necessary to accurately match motored pressure data as well as to match the total energy released during the main combustion event.

The effect of wall heat transfer was accounted for using the Annand correlation (Annand, 1963) with the mean piston speed as the characteristic velocity and air properties for thermal conductivity and viscosity. The wall temperature was chosen to be 500 or 550K for the 1000 and 2000 r/min conditions, respectively, due to the high load operation of the engine (and expected high piston temperature); motored calculations also required the high wall temperature to match the experimental pressure trace.

The combustion rate through the deflagration process was modeled by transferring mass from the unburned to burned regions. The burned region was given a small mass at intake valve closing (IVC) at the adiabatic flame temperature conditions, which was sufficient to ensure that the unburned mass would fully combust when transferred to the burned region. The rate of mass transfer from the unburned regions was fixed by a Wiebe function. The Wiebe function parameters were set manually on a case-by-case basis to get a good match to the measured pressure data. As the focus of this work was on the pre-spark heat release, this method was deemed sufficient.

2.2 Chemical models

Two chemical kinetic mechanisms were tested. The first mechanism was a multi-component skeletal mechanism developed by Ren et al. (Ren, et al., 2017), and will be referred to in subsequent plots as RK (based on the first two authors). The mechanism includes 178 species and 854 reactions, and was developed to facilitate fast computation of a wide range of distillate fuels in computational fluid dynamics codes. The second mechanism tested was a detailed mechanism from Lawrence Livermore National Laboratory (LLNL) with 2027 species and 8720 reactions. This mechanism is based on the publicly available gasoline surrogate model from LLNL (Mehl, et al., 2011), but this version was obtained from LLNL via personal communication as it is being updated to include new components that are of interest to the Co-Optima initiative. This mechanism also includes chemistry that describes the interaction of nitrogen oxide (NO) with the low temperature fuel chemistry, but in the current case the effect of NO from the residual gas was not examined.

The RK mechanism was able to compute a single cycle in approximately 60 seconds on a desktop computer, but the LLNL mechanism took approximately 5 hours. The slow computations for the LLNL was a function of both the large number of species and stiffness caused by the transfer of mass between the two zones. As a result, the majority of the preliminary computational scoping activity took place with the RK model.

3. Results

3.1 Experimental results

Figures 1 and 2 show the experimental heat release rates for three intake temperatures at 1000 and 2000 r/min, respectively. The axes ranges have been chosen to highlight the region near spark timing, which is shown as the vertical dashed line in these and all subsequent figures; the main heat release occurs later at a larger magnitude. The three conditions chosen correspond to different levels of pre-spark heat release. The leftmost columns of both figures, at the lowest intake temperature, show little to no heat release before the ignition timing. As the intake temperature was increased, heat release is observed in the bulk gas before the ignition timing. At the highest temperatures (the rightmost column), fully expressed pre-spark heat release is seen, i.e., the energy release starts and then as the bulk gas heats the reactions slow and restrain the heat release. The effect of increased engine speeds is twofold. First, the higher speed requires a higher temperature to achieve qualitatively similar pre-spark heat release; for example fully expressed pre-spark heat release is seen at 110 ºC at 1000 r/min and 140 ºC at 2000 r/min. In addition, the total amount of heat release in the pre-spark heat release (the integral under the curve) is seen to decrease with higher engine speed. This is assumed to be the result

of the lower residence time spent in thermodynamic regions that give rise to low temperature heat release. Consistent with the previous results of (Szybist & Splitter, 2017), further increases in intake temperature do not increase knocking propensity and further retarding of combustion phasing with increasing intake temperature is not required.

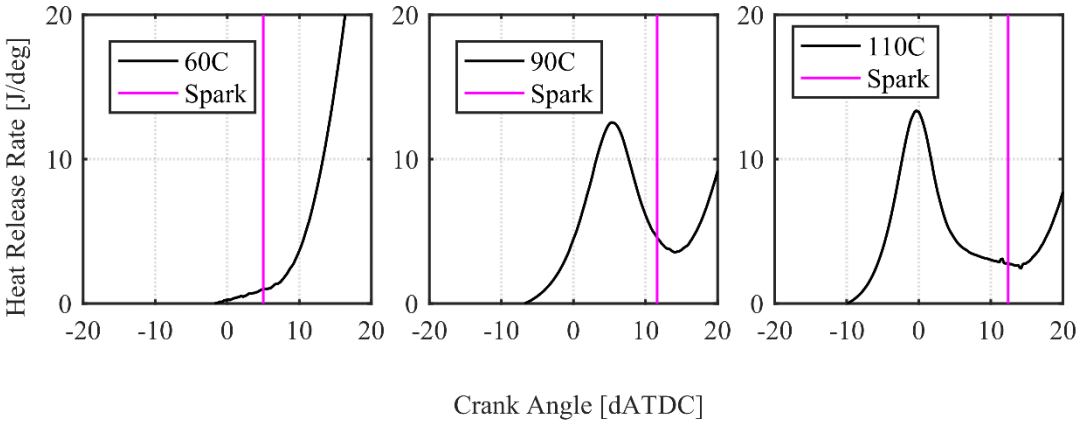

Fig 1. Black line indicates experimental iso-octane heat release at 1000 rpm for 60, 90, and 110ºC intake temperature

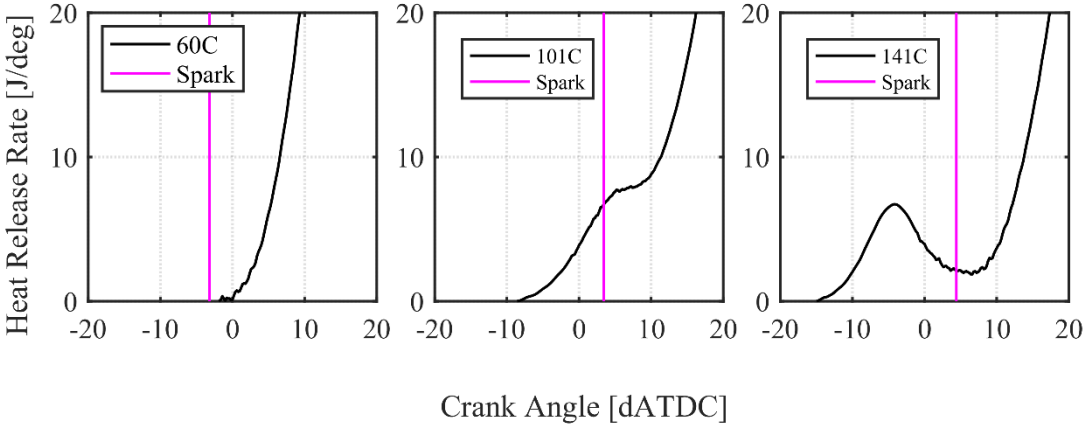

Fig 2. Black line indicates experimental iso-octane heat release at 2000 rpm for 60, 101, and 141ºC intake temperature

The experimental IVC temperature, which differs from the intake temperature set point, was found from an ideal gas calculation that used the known IVC volume and the measured delivered mass and an estimate of the residual mass in the cylinder using the approach by (Fox, et al., 1993). The correspondence between the two temperatures is seen for both speeds in Fig. 3. A line of IVC temperature to intake temperature with a 1:2 slope is plotted for reference. It can be seen that a 2 K change in intake temperature nominally gives a 1 K change in temperature at IVC. This relationship will be used when comparing the model results, which are based on IVC temperature, to the experimental results, which are referred to based on their intake temperature. It is noted that this is an empirical result that is specific to the current setup, but similar effects, albeit with different magnitude, are universal.

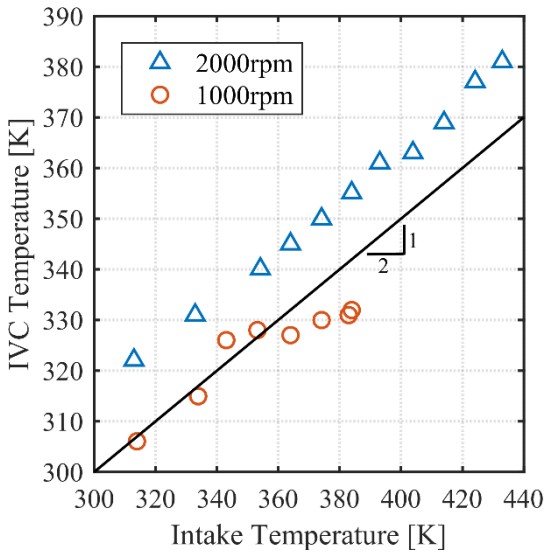

Fig 3. Comparison of IVC temperature estimation to intake temperature for 1000 r/min (circles) and 2000 r/min (triangles). A 1:2 line is shown for reference.

3.2 Model heat release results

The absolute temperature of the trapped charge at IVC calculated from the experimental data has some (absolute) uncertainty. Therefore, to get a fair comparison for the model, a condition at the middle of the intake temperature sweep was chosen for finding an appropriate IVC temperature to use in the simulations (90°C at 1000 r/min and 100°C for 2000 r/min, see the center figures in Figs. 1 and 2). At these conditions the IVC pressure was fixed at the experimental value and the IVC temperature was swept in 5 K increments. The metric used to choose a best match, deemed the appropriate IVC temperature, was the phasing of the low temperature, pre-spark heat release. The RK mechanism was used for these calculations. Figure 4 shows the predicted heat release rate of the unburned charge (note, this does not account for the heat release associated with the main combustion event) at several IVC temperatures relative to the experimental data (purple dashes). According to Fig 4, 365 K was deemed the correct IVC temperature for the 1000 r/min data at an intake temperature of 90 °C. A similar procedure was followed for 2000 r/min.

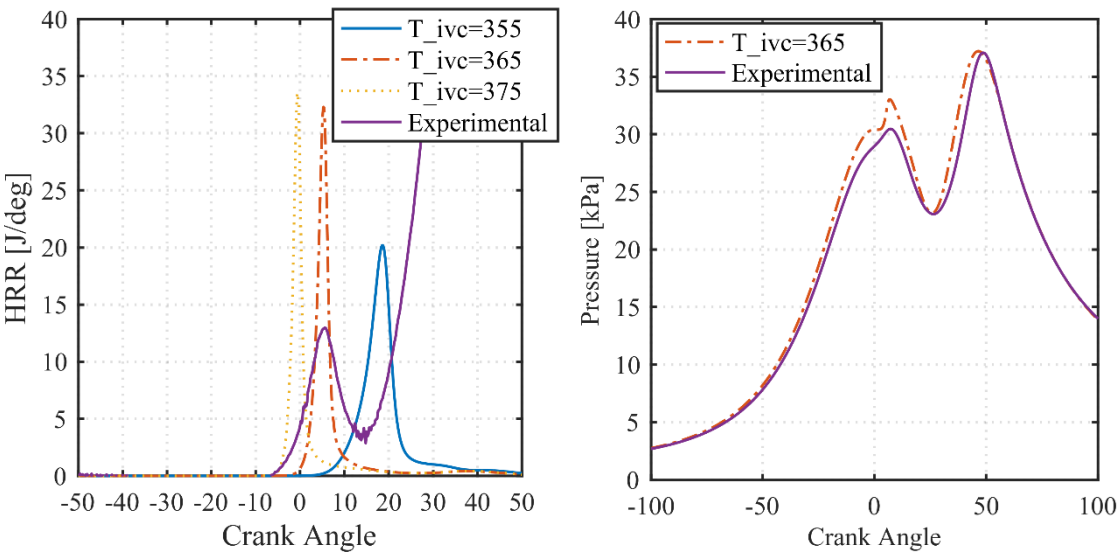

Fig 4. Comparison of experimental heat release with model heat release for T_IVC= 355, 365, 375K at 1000 r/min and 90ºC intake temperature

Calculations of the intake temperature sweep were performed by starting with the matched condition as the base. Because the measurements were performed with a 10 K intake temperature increment, a 5 K IVC temperature increment was used for the calculations based on the results of Fig. 3. In addition, the trapped mass was assumed to be the same as from the matched condition for changes in intake temperature, which in turn prescribed the IVC pressure. Using this approach, IVC temperature sweeps were simulated using both mechanisms. Figure 5 shows the heat release rate of the RK and LLNL mechanisms relative to experimental data for iso-octane at 1000 r/min. The two mechanisms both compare well to the experimentally observed trends. The phasing of the pre-spark heat release predictions is found to track the intake temperature changes well. The RK mechanism tends to show a higher and narrower peak compared to the LLNL mechanism, but both mechanisms show a skewness that is seen in the experimental data. In addition, the width of the predicted pre-spark heat release is substantial in spite of the omission of either composition or thermal stratification in the model.

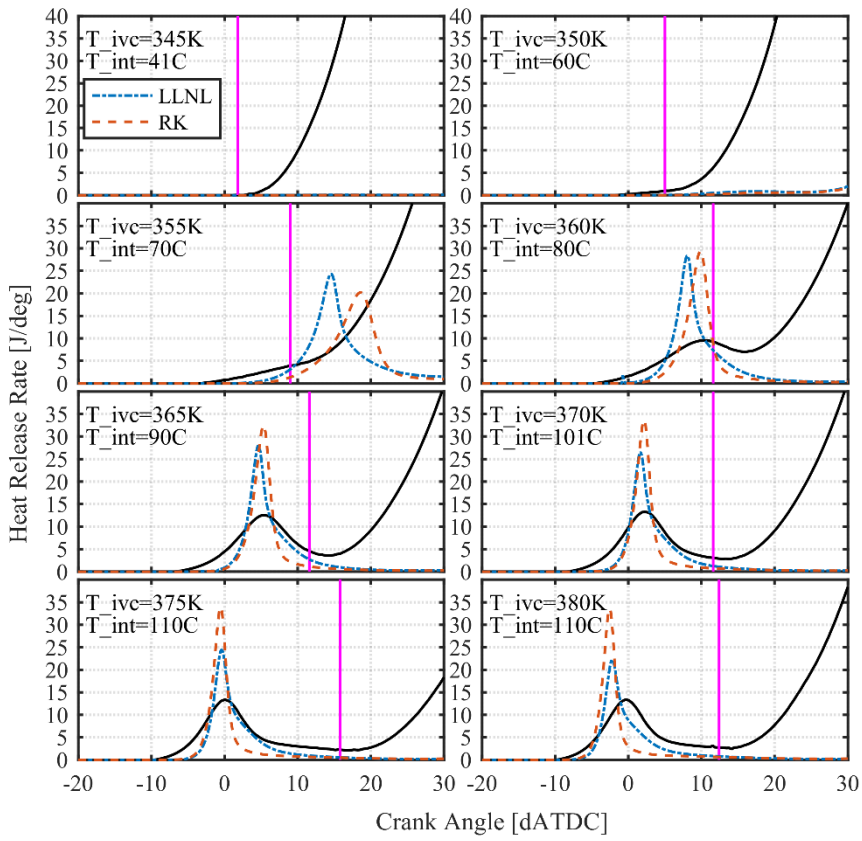

Figure 5. Comparison of experimental, black line, and colored lines, heat release for the full sweep of intake temperatures at 1000 r/min. Both kinetic mechanisms are shown and the IVC temperature was varied in a 1:2 relation to the intake temperature

The computational results for the 2000 r/min data are compared to the expermental results in Fig. 6. At 2000 r/min, the RK mechanism mechanism is seen to do a better job of matching the phasing of the pre-spark heat release to the experimental data at and above 90ºC intake where it is visible in the experimental data. The LLNL mechanism tends to have a later onset of pre-spark heat release at the high temperatures, and a lower peak magnitude and extended duration. The model results in Fig. 6 show an interesting result. At the lower intake temperautres, the unburned zone for both models undergoes some chemical change with heat release. This is masked in the experimental results because of the significantly larger magnitude of the deflagration heat release. This chemical change in the end gas could have a significant effect on both the deflagration rate as well as the knock propensity of the end gas. Finally, at 2000 r/min the pre-spark heat release magnitude seen to vary with intake temperature. The experimental results show a peak value of 7.5 J/deg at 110 ºC intake temperature,

but only 5 J/deg at 160 ºC. Both chemical mechanisms show a similar tred of decreasing pre-spark heat release with increasing intake temperature.

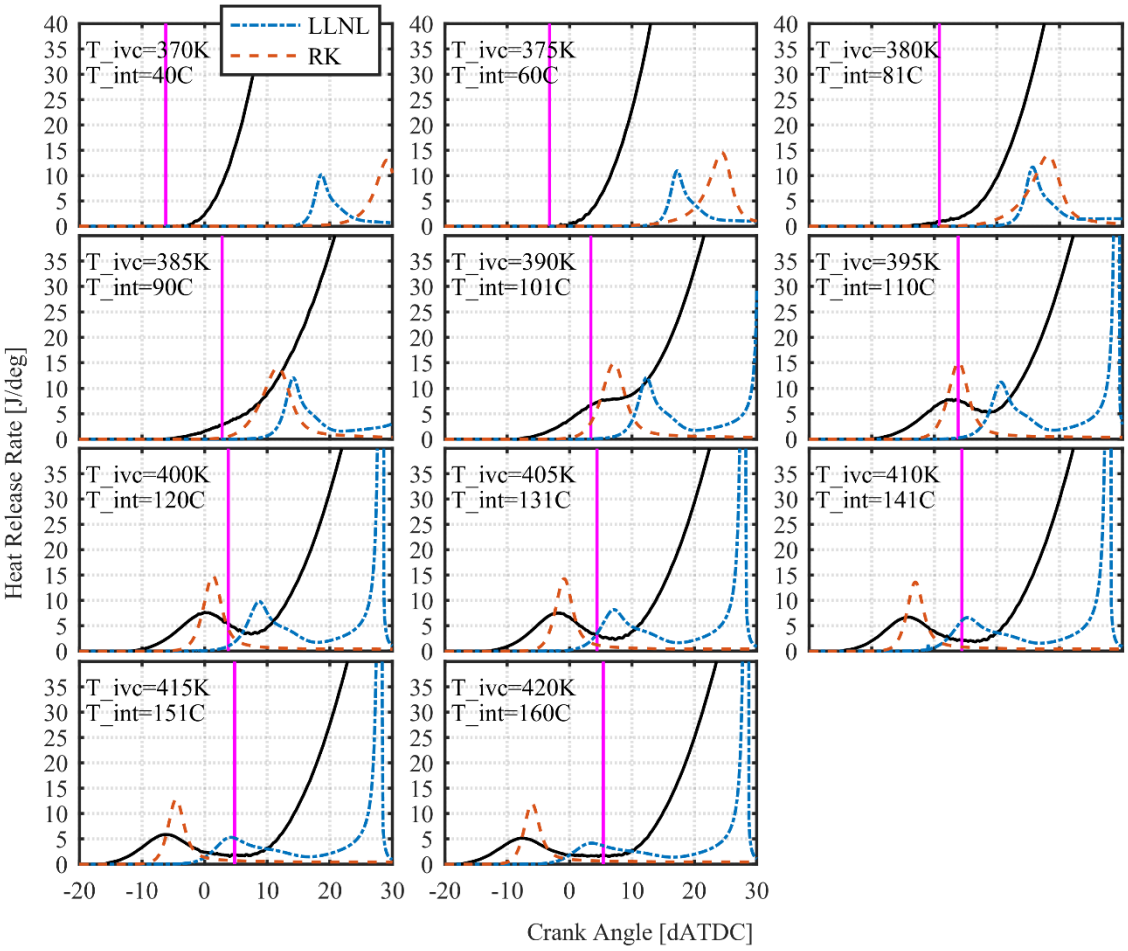

Fig 6. Comparison of experimental, black line, and model, colored lines, heat release for the full sweep of intake temperatures at 2000 rpm. Both kinetic mechanisms are shown and the IVC temperature was varied in a 1:2 relation to the intake temperature. The vertical line represents the experimental ignition timing.

3.3 Discussion of model results

The model results can be used to explore the conditions of the unburned mixture during the combustion event. Figure 7 shows the unburned gas state on P-T axis, with ignition delays shown in the background; ignition delay was defined as a 50 K temperature rise for a constant pressure reactor calculation. The three temperature conditions shown, from low to high, represent cases of no, partially expressed, and fully expressed pre-spark heat release (see Fig. 6). The RK mechanism was used for these calculations. The pressure and temperature increase during the compression stroke, as expected. The 375 K condition reaches the spark time (denoted with a star in the figure) at a time when the ignition delay is approximately 3 ms, which is long enough that no autoignition takes place. A similar situation is observed at 390 K, but shortly after spark timing, the temperature increases from approximately 750 K to 820 K due to LTHR from the unburned fuel. The ignition delay at 820 K is longer than at 750 K due to the negative temperature coefficient (NTC) behaviour of iso-octane, and thus the mixture becomes unreactive. For the 390 K condition, the pressure rise due to deflagration heat release first increases then decreases pressure and temperature up to 50 dATDC (shown with the diamond marker) with no subsequent energy release. The 420 K condition, however, compresses to a region of low ignition delay before spark timing, and autoignites (seen by the temperature increase). Similar to the 390 K data, the increased temperature moves the state into regions of relatively long ignition delay, avoiding knock. The 375 K data show an interesting effect. Even though there is no pre-spark heat release, there is heat release and a chemical change in the end gas (see Fig. 6) about 25 dATDC. This heat release causes

the temperature to deviate from the expected (nearly) isentropic condition, as seen by the inflection point in Fig. 7. A standard heat release analysis would not be able to pick up this effect because the magnitude is small compared to the deflagration heat release. At 375 K, the end gas spends an extended amount of time in regions of low ignition delay. In fact, small perturbations of the operating conditions would cause the end gas to autoignite in the model, illustrating sources of instability and abnormal combustion that contribute to end gas knock in actual operation.

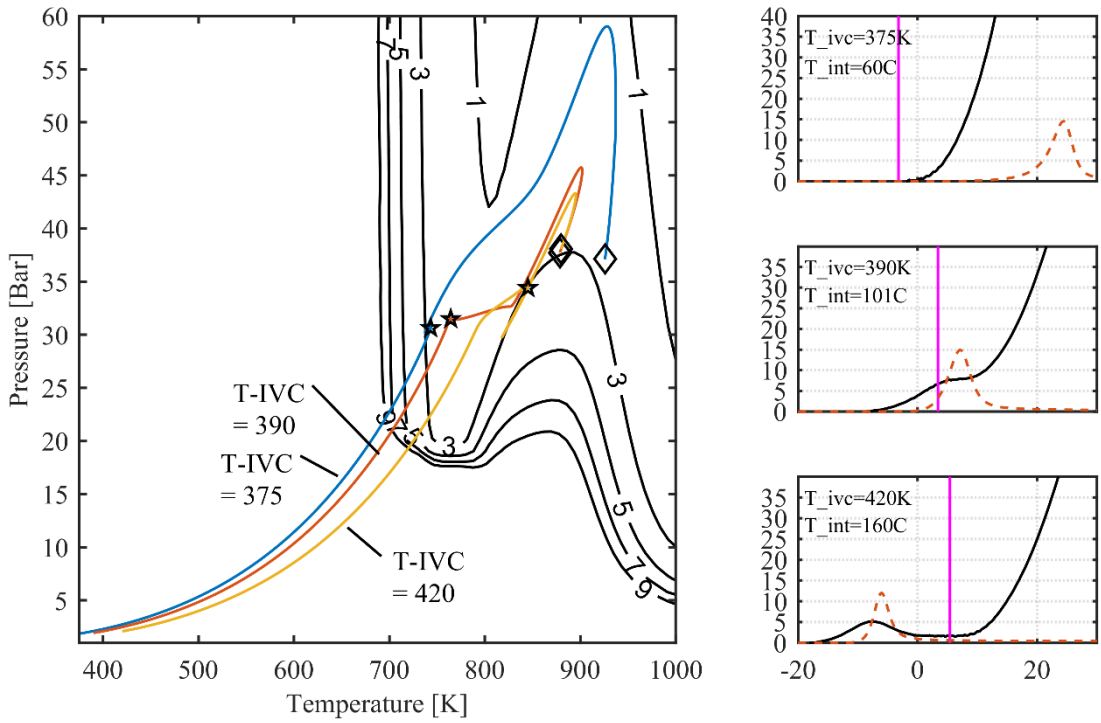

Fig 7. End gas state for 2000 r/min condition, where black lines in the right-hand plots are experimental data, dashed lines are modeled heat release with the RK mechanism, magenta line indicates spark timing. In the left-hand plot black contour lines indicates the ignition delay in [ms] as defined by a 50K temperature rise, are shown in the background, colored lines are corresponding experimental heat release for conditions as labeled and indicated in right hand figures. The star in the left-hand figures represents the spark timing, and the diamond 50 dATDC.

Given the good agreement between the RK model and the experimental results, the model was exercised to develop a more general understanding of when pre-spark heat release may be important. The model was iterated such that the pre-spark heat release peaked within ±1 crank angles of TDC (this is an arbitrarily chosen timing, but other values would give rise to similar results) by adjusting the IVC temperature at a given IVC pressure and engine speed. The required temperature is shown at the left in Fig. 8 for engine speeds ranging from 1000 to 3000 r/min. A retarded combustion phasing (peak pressure location ~40dATDC) was used for all cases. It can be seen that, as expected, higher IVC temperatures are required to achieve the TDC heat release when the engine speed increases. The temperature requirement is weakly dependent on the boost level (IVC pressure). Additionally, the heat release from the unburned zone was integrated over the time window from -10 to 10 crank angle degrees, which covered the full extent of the pre-spark heat release condition. The integrated heat release is shown in Fig. 8 at the right. It can be seen that as the engine speed increases, the amount of pre-spark heat release decreases. This is assumed to be due to the fact that the gas mixture spends less residence time in the regions where low temperature, finite-rate chemistry releases heat. In general, at high engine speed the IVC temperature requirement to experience pre-spark heat release is probably excessive and the subsequent amount of energy release is modest in magnitude. Both of these results are consistent with the findings of Figs. 1, 2, 5, and 6.

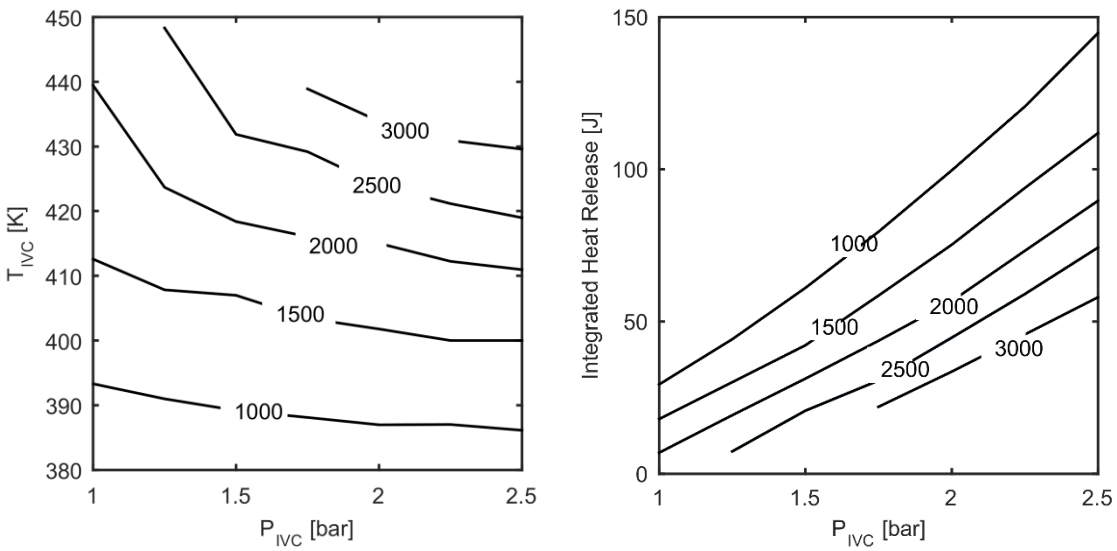

Fig 8 Required IVC temperature (left) and amount of integrated heat release (right) for different IVC pressures (boost levels) and engine speeds (contours in r/min). The conditions shown all had a low temperature heat release event that peaked at TDC

The combined ramifications of this work on knock and fuel specific effects are currently under investigation, but the present findings highlight that fuel kinetics and low-temperature chemistry are expressed in boosted SI engines at even moderate to low boost pressures with mildly elevated intake temperatures. This could be a significant effect in modern engine operating conditions, and could be used for decoupling combustion phasing retard for knock mitigation from increased IVC temperature at some conditions.

Conclusions

A series of experiments were performed under boosted conditions wherein pre-spark heat release was observed. The experiments included two speeds, a variety of fuels, and a wide range of intake temperatures. The current experimental results were analysed for only one for the fuels, which was modelled using a three-zone kinetic model that included an inert crevice and the unburned and burned zones. Two chemical kinetic mechanisms were investigated: a skeletal mechanism with 178 species and a detailed mechanism with 2027 species. In order to avoid issues associated with the assignment of a surrogate representation, only the isooctane-fuelled experiments were modelled. The IVC temperature was adjusted at one condition to match pre-spark heat release phasing, and the experimental result of a 1:2 relation between IVC and intake temperature was used to compare model to experimental results.

Both mechanisms predicted the occurrence of pre-spark heat release. At 1000 r/min, both mechanisms correctly predicted the change in phasing of the pre-spark heat release with intake temperature variation. At 2000 r/min, the detailed mechanism tended to predict more retarded pre-spark heat release timings that lagged the observed experimental results; the skeletal mechanism, however, faithfully tracked the experimental results. Detailed end gas conditions were compared to ignition delay contours for cases with varying levels of bulk gas heat release prior to ignition. Notably, even the case with no pre-spark heat release showed heat release in the bulk gas. The skeletal mechanism was used to explore conditions where pre-spark heat release would occur. The model results show that the engine speed plays a significant role in pre-spark heat release. Higher engine speeds require higher IVC temperatures for pre-spark heat release to occur, and at the higher speeds the amount of energy released is reduced.

Acknowledgement

This research was conducted as part of the Co-Optimization of Fuels and Engines (Co-Optima) initiative sponsored by the US Department of Energy Office of Energy Efficiency and Renewable Energy and Bioenergy Technologies and Vehicle Technologies Offices. Co-Optima is a collaborative project of multiple national laboratories initiated to simultaneously accelerate the introduction of affordable, scalable, and sustainable biofuels and high-efficiency, low-emission vehicle engines. Special thanks to program managers Kevin Stork, Gurpreet Singh, Leo Breton, and Mike Weismiller.

We would also like to thank Bill Pitz, Marco Mehl, and Scott Wagnon for providing access to the pre-release version of the Co-Optima gasoline surrogate chemical kinetic mechanism.

References

Annand, W., 1963. Heat Transfer in the Cylinders of Reciprocating Internal Combustion Engines. *Proceedings of the Institution of Mechanical Engineers,* Volume 1, pp. 973-996.

Curran, H., Gaffuri, P., Pitz, W. & Westbrook, C., 1998. A Comprehensive Modeling Study of n-Heptane oxidation. *Combustion and Flame,* July.114(1-2).

Curran, H., Gaffuri, P., Pitz, W. & Westbrook, C., 2002. A comprehensive modeling study of iso-octane oxidation. *Combustion and Flame,* May.129(3).

Fox, J., Cheng, W. & Heywood, J., 1993. A Model for Predicting Residual Gas Fraction in Spark-Ignition Engines. *SAE Technical Paper 931025.*

Leppard, W., 1990. The Chemical Origin of Fuel Octane Sensitivitiy. *SAE Technical Paper 902137.*

Mehl, M., Pitz, W. J., Westbrook, C. K. & Curran, H. J., 2011. Kinetic modeling of gasoline surrogate components and mixtures under engine conditions. *Proc. Comb. Inst.,* 33(1).

Najt, P. & Foster, D., 1983. Compression-Ignited Homogeneous Charge Combustion. *SAE Technical Paper 830264.*

Ren, et al., 2017. A Multi-Component Wide Distillation Fuel (Covering Gasoline, Jet Fuel, and Diesel Fuel) Mechanism for Combustion and PAH Prediction. *Fuel,* Volume 208, pp. 447-468.

Rooney, et al., 1991. Knock Characteristics of Liquid and Gaseous Fuels in Lean Mixtures. *SAE Technical Paper 912311.*

Splitter, D., Pawlowski, A. & Wagner, R., 2016. A Historical Analysis of the Co-evolution of Light-duty Fuels and Engines. *Frontiers in Mechanical Engineering,* Volume 1.

Szybist, J. & Splitter, D., 2017. Pressure and Temperature Effects on Fuels with Varying Octane Sensitivity at High Load in SI Engines. *Combustion and Flame,* Volume 177, pp. 49-66.

Szybist, J. & Splitter, D., 2018. Understanding Chemistry-Specific Fuel Differences at a Constant RON in a Boosted SI Engine. *Fuel,* Volume 217, pp. 370-381.

Westbrook, C., Mehl, M., Pitz, W. & Sjoberg, M., 2016. Chemical kinetics of octane sensitivity in a spark-ignition engine. *Combustion and Flame,* In Press. Accepted May 2016.

Yamakawa, M. et al., 2011. Combustion Technology Development for a High Compression Ratio SI Engine. *SAE Int. J. Fuels Lubr.,* 5(1).